Rafal P. JASTRZEBSKI[1], Katja HYNYNEN[2], Alexander SMIRNOV[3], Olli PYRHÖNEN[4]

Lappeenranta University of Technology (1,2,3,4)

Influence of the drive and dc link generated disturbances on an AMB control system

Abstract. *The work focuses on experimental and theoretical examination of the influence of the distortion signals generated by the inverter and the active magnetic bearing (AMB) dc link voltage on an AMB control system. These low-frequency disturbances may result in performance degradation or lead to an unstable system. The analysis and measurements are performed on an AMB system controlled by an H_∞ controller. The studied signals include positions and currents in 5DOF, AMB dc link voltage, drive currents, and acceleration of the stator frame.*

Streszczenie.. *W tej pracy opisano doświadczalne i teoretyczne badania wpływu napędu i zaburzeń napięcia zasilacza na system sterowania łożysk magnetycznych. Te niskoczęstotliwościowe zakłócenia mogą powodować obniżenie sprawności lub utrate stabilności systemu. Analiza i doświadczenia prowadzone były dla systemu zawieszenia ze sterowaniem odpornym. Mierzone sygnały obejmowały położenia i prądy w systemie zawieszenia o 5 stopniach swobody, napięcie zasilania łożysk, prądy napędu i przyspieszenie obudowy. (**Wpływ napędu i zaburzeń napięcia zasilania na system sterowania łożysk magnetycznych**).*

Keywords: magnetic levitation, active magnetic bearings, drive train, rotating machines.
Słowa kluczowe: zawieszenie magnetyczne, aktywne łożyska magnetyczne, elementy przeniesienia napędu, maszyny wirnikowe.

Introduction

The need for safe operation in difficult environments and energy saving in high-speed drive train requires an alternative solution to traditional bearings. These needs can be met and the limitations of traditional mechanical bearings can be overcome by applying magnetically levitated rotors. Because of a contactless, lubricant-free operation principle, the low-loss active magnetic bearings (AMBs) are superior to the traditional bearings.

Now, there is a question about the limitations and difficulties in applying the active magnetic bearing technology to rotating machines with inverters. The answer will facilitate design decisions, suggest active control solutions that can compensate some of the physical and hardware limits, and extend the industrialization and applicability of the technology. Schweitzer [1,2] studied general physical limits, such as load, size, stiffness, temperature, precision, speed, losses, and dynamics. The limitations can be regarded from the AMB hardware point of view. The limitations such as non-ideal actuators (limited power and bandwidth) and sensors, bending modes of elastic rotors, elastic properties of the supporting structures and foundations, and high temperatures have been studied before [3,4,5,6].

In AMB systems, the controller has to be designed carefully to enable stable operation and high performance. The rotor suspension on AMBs is an unstable, nonlinear, and multiple-input multiple-output control system, which changes its dynamics over time and for different rotational speeds. The high-performance and high-precision control requires accurate models of the controlled process and good disturbance rejection. The need for many measurement and transmission channels makes the control system particularly vulnerable to the external noise and disturbances. In particular, the robustness of the magnetic suspension with respect to variation of plant parameters and disturbances coming from various sources, such as the drive, load, and base should be validated.

This work extends the previous results with the experimental and theoretical examination of the influence of the distortion signals and noise generated by the inverter and the dc link voltage on the AMB control system. These disturbances act in the low-frequency region (300 Hz and less) and within the bandwidth of AMB actuators. Therefore, they might result in performance degradation or lead to unstable system. The machine under test was originally a solid rotor induction motor for general industrial high-speed applications with the rated speed 12000 rpm by Rotatek Finland Oy. The custom-built AMB setup consists of two radial actuators and one axial actuator supporting a 42 kg rotor (Fig. 1). The rotor is of a long rotor type without a significant gyroscopic effect, and the machine is subcritical. According to the finite element model calculations and experimental modal analysis [7] the first three bending modes of the rotor are at 260 Hz, 539 Hz, and 952 Hz. The damping ratios of 1-3 flexible modes are 0.0041, 0.0022, and 0.0043, respectively. The first and the second mode pose a threat for the control system because they can be excited by the AMB actuators. The airgap of the AMBs is about 500 μm. The tested controller is a model-based centralized H_∞ controller [8]. The measured signals comprise the AMB positions and currents in 5DOF, AMB dc link voltage, drive currents, and acceleration signals collected at the stator frame.

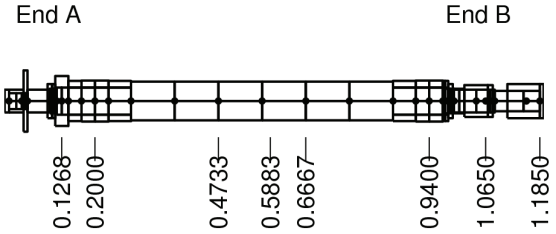

Fig.1. Rotor of the test rig with marked locations (distance in m from the left): radial sensor plane, radial AMB, beginning of the drive terminal, centre point mass of the rotor, end of the drive terminal, radial AMB, and radial sensor plane. At the end A there is an axial AMB disc with its actuator and sensor.

AMB dc link voltage ripple

The AMB dc link voltage applied to the current control of the studied laboratory prototype comprises a 1410 µF dc link capacitor and a three-phase uncontrolled diode bridge rectifier. A variable autotransformer by Transpower (R16-260) has been used to feed power at variable voltage.

The application of uncontrolled diode rectifier results in the 300 Hz voltage ripple, that is, a 6th harmonic of the fundamental of f_0=50 Hz. For the rectifier without capacitance, the Fourier series expansion of the ac voltage component [9] is

$$v_{\text{out}} = -\frac{3\sqrt{3}}{\pi} V_{\text{m}} \sum_{k=1}^{\infty} \frac{2}{36k^2 - 1} \cos\left(6k\omega_0 t\right), \tag{1}$$

where V_m is the phase voltage, t is time and $\omega_0=2\pi f_0$. Figure 2 presents the measured voltage ripple during the levitation for the dc link voltage v_{150}=150V when supplied from the variable autotransformer. The frequency spectrum of the dc link voltage ripple is presented in Fig. 3. After the 6th harmonic, the next highest amplitude corresponds to the 2nd harmonic at 100 Hz. This can be explained by the not purely sinusoidal voltages of the power supply system during the experiments. Moreover, the working AMB switching servodrives also affect the resulting dc link voltage.

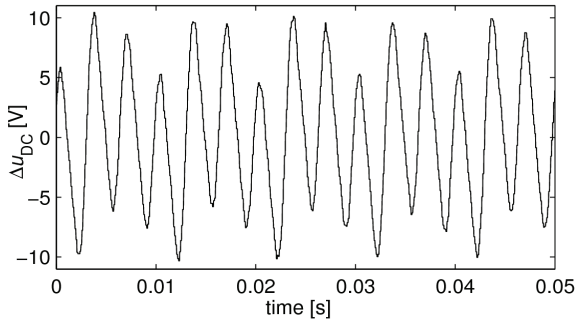

Fig.2. Measured AMB dc link voltage ripple when AMBs turned on

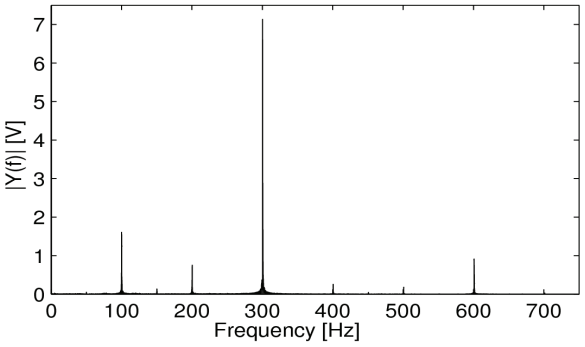

Fig.3. Amplitude spectrum of the measured AMB dc link voltage

The voltage ripple at f_{300}=300 Hz propagates to the measured AMB coil currents as seen in Figs. 4, 5, and 6.

The relation between the coil current $i(t)$ and the applied voltage command $v(t)=v_{150}\cos(\omega t)$ for the ideal AMB coil inductance L_{AMB} can be expressed as

$$i(t) = L^{-1}\left\{\frac{1}{sL_{\mathrm{AMB}}} L\{v_{150}\cos(\omega t)\}\right\} = \frac{v_{150}}{L_{\mathrm{AMB}}\omega}\sin(\omega t), \tag{2}$$

where $L\{\odot\}$ and $L^{-1}\{\odot\}$ are the Laplace transform and its inverse. The maximum voltage command amplitude is equal to the dc link voltage v_{150}=150V. The amplitude of the resulting current is inversely proportional to the frequency of the input voltage command ω, which limits the bandwidth of the actuator and the amplitude of the coil current. According to Eq. (2), the actuator can produce the sinusoidal coil current with 1 A amplitude at 568 Hz using the voltage command of amplitude equal to 150 V.

Using the cosine trigonometric identity we rewrite the input voltage for dc link modulation

$$\begin{aligned} v(t) &= v_{150}\left(1 + S_{\mathrm{c}}\cos(\omega_{300}t)\right)\cos(\omega t) = \\ &= v_{150\mathrm{V}}\cos(\omega t) + \frac{v_{150}S_{\mathrm{c}}}{2}\cos((\omega+\omega_{300})t) + , \\ &+ \frac{v_{150}S_{\mathrm{c}}}{2}\cos((\omega-\omega_{300})t) \end{aligned} \tag{3}$$

where S_c is the modulation index. $\omega_{300}=2\pi f_{300}$. As an example, the sinusoidal excitation voltage signals at ω=350 Hz and 250 Hz result in the sinusoidal current signal at 50 Hz. In general, disturbances at lower frequencies are more dangerous for the AMB control than at higher frequencies.

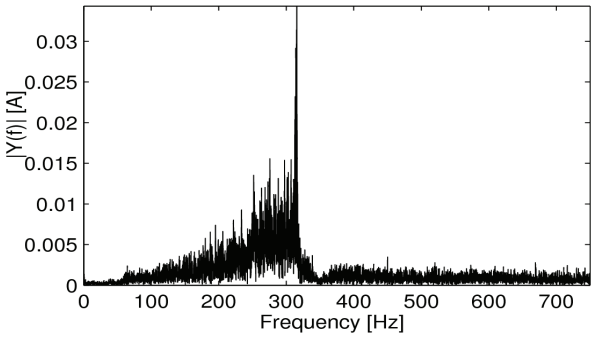

Fig.4. Amplitude spectrum of the measured positive coil current for the *z* direction

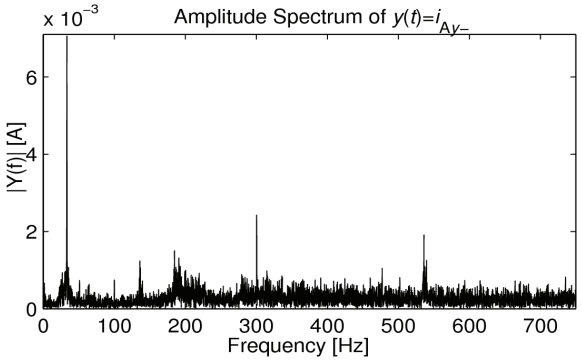

Fig.5. Amplitude spectrum of the measured positive coil current for the *y* direction at the end A (33 Hz excitation in the drive current)

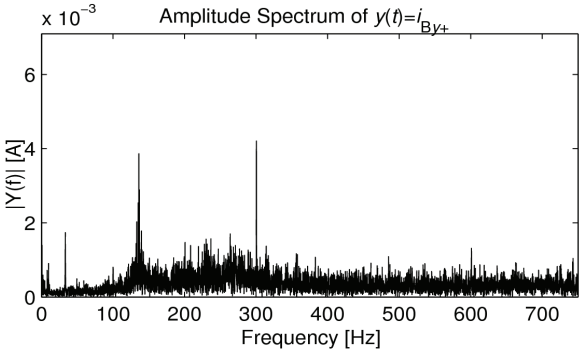

Fig.6. Amplitude spectrum of the measured positive coil current for the *y* direction at the end B (33 Hz excitation in the drive current)

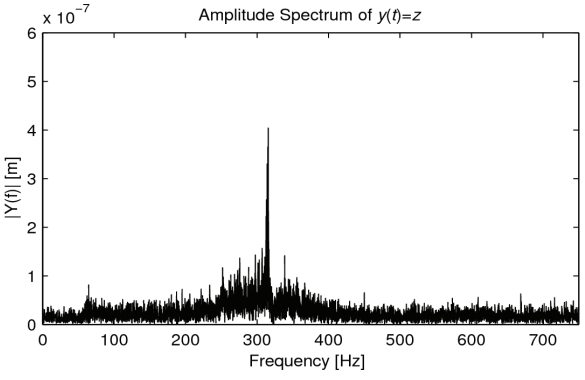

Fig.7. Amplitude spectrum of the measured position displacement in the *z* direction

The 300 Hz harmonic is visible in the measured currents for the both radial and axial directions (Figs. 4, 5, and 6). This 300 Hz current ripple seems to be exciting vibrations in the *z* direction close to 300 Hz as seen in the axial position signal (Fig. 7) but not in the radial displacements (Figs. 8 and 9). The possible explanation is given in Fig. 10. The presented frequency response function was calculated using a smoothed empirical transfer function estimate (ETFE).

The ETFE is the simplest nonparametric identification method. It is obtained as the ratio of the output Fourier transform to the input Fourier transform. At 324 Hz there is a structural resonance in the transfer function. This resonance could be shifted by the controller and could explain the oscillations in Fig. 7.

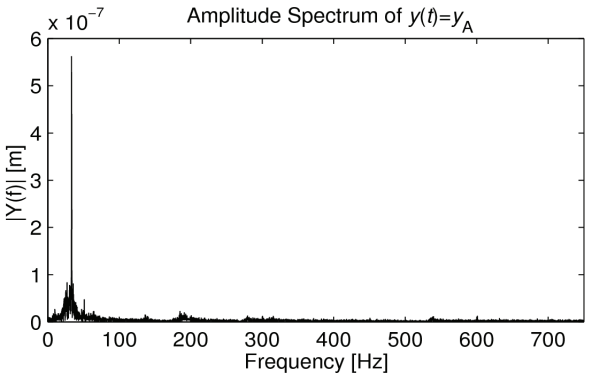

Fig.8. Amplitude spectrum of the measured position displacement in the *y* direction at the end A

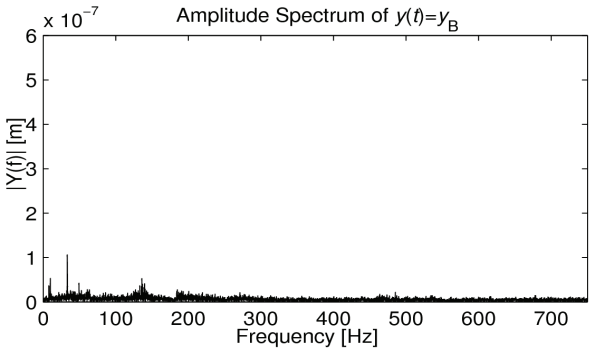

Fig.9. Amplitude spectrum of the measured position displacement in the *y* direction at the end B

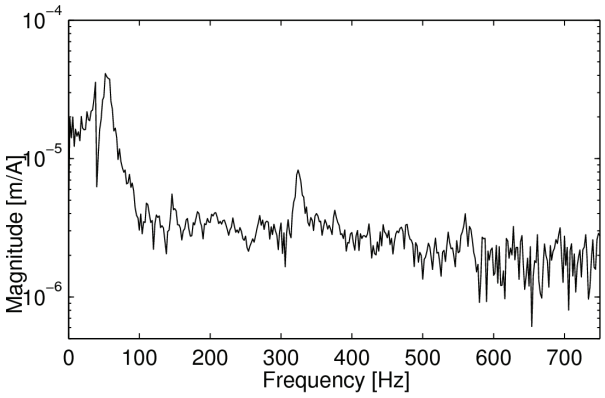

Fig.10. Measured frequency response of the plant from the control current i_{cz} to the axial displacement *z*

Figure 11 shows the rotor response obtained using stepped sine excitation with amplitudes of the control current varying from 50 mA to 500 mA for different frequency ranges. As explained by eq. (2) and (3), the 300 Hz voltage ripple can produce low frequency rotor disturbances (below 100 Hz) in the presence of the other excitation signals (e.g., from the controller). In Fig. 11, an amplitude modulation effect in the rotor response is marked by red arrow and 1. Additionally in the Fig. 11, there are visible effects of the network disturbance about 50 Hz. The low frequency peaks at 78 Hz and 90 Hz (pointed to by the red arrow and 2) are odd harmonics of 26 Hz and of 30 Hz (3⊙26=78 and 3⊙30=90).

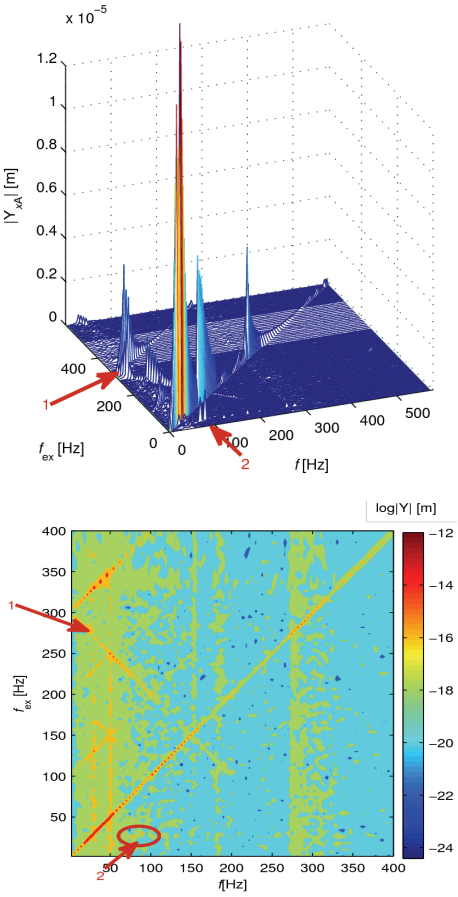

Fig.11. Measured rotor response to the AMB control current (excitation at f_{ex}) at the end A in *x* direction

The frequency of 300 Hz is far enough from the first bending mode of the rotor. However, because of the modulation effect the dc link voltage ripple can leading to oscillations at frequencies below 100-150 Hz and instability.

The amplitude of the voltage ripple can be reduced by using a larger capacitor in the dc link, an LC filter after the rectifier or the control method, which would update the voltage commands according to the dc link voltage measurement. For the motor control, an example of such a control method is direct torque control (DTC) [10].

In general, the pulse width modulation (PWM) and switching in the AMB actuators produce high frequency current ripple and electromagnetic disturbance. The switching frequency of the studied AMB actuators is 40 kHz. The effect of this electromagnetic disturbance can be minimized by the proper protection of the control electronics and measurements and among other solutions by reducing the dc link voltage level. The level of optimal dc link voltage is a compromise between the increased current ripple (because of the switching amplifiers) and a voltage saturation of the current actuators (bandwidth limitation).

A detailed analysis of the influence of the dc link voltage level on the AMB control and the in-depth study of reduction of the dc link voltage disturbance are out of the scope of this work.

Influence of the drive

The influence of the ABB high-performance machinery drive ACSM1 on the custom built AMB system is tested when using the stator of the motor which has too great an inner diameter with respect to the rotor outer diameter. In other words, there are no rotor laminations present. In such a test rig, the stator of the motor does not generate sufficiently strong magnetic forces on the rotor to enable rotation. The AMB system currents and positions are recorded together with the 3-phase-motor currents and acceleration of the stator frame. During testing bout 20 to 55 A peek-to-peek drive phase currents and from 5 Hz to 500 Hz speed references are applied. The amplitude is smaller for the lower frequencies and increases with the frequency up to 55 A at 500 Hz.

At first, the operation of the tested AMB laboratory setup was not stable in the presence of the drive generated disturbances if the power and measurement cables ware not shielded. Therefore the suitable shielding of the control electronics and proper grounding are very important prior to testing.

For example, the 33 Hz fundamental frequency of the drive is visible in the radial current and position signals in Figs. 5, 6, 8, and 9. The observed low-frequency vibrations (peeks 33 Hz and 66 Hz) using accelerometers (Fig. 12 and Fig. 13) result from vibrations induced by the drive currents.

For the analysis, it is convenient to reduce the three-phase currents from three to two degrees of freedom. Considering the projection of the space vector on the α (real) axis, the peak-to-peak current is

$$i_\alpha = \frac{2}{3} i_u - \frac{1}{3} i_v - \frac{1}{3} i_w , \tag{4}$$

where i_u, i_v, and i_w are the measured phase currents. Figure 14 shows the amplitude spectrum of the i_α. for the 33 Hz speed reference.

The highest vibration amplitude peak (Figs. 12 and 13) is found at twice the frequency of the rotating flux vector. This is because of the frame own frequency response and the location of the acceleration sensors. The drive-induced disturbances can propagate to the AMB control system through the vibrations of the base, machine tubing, and stator frame and through the electromagnetic fields.

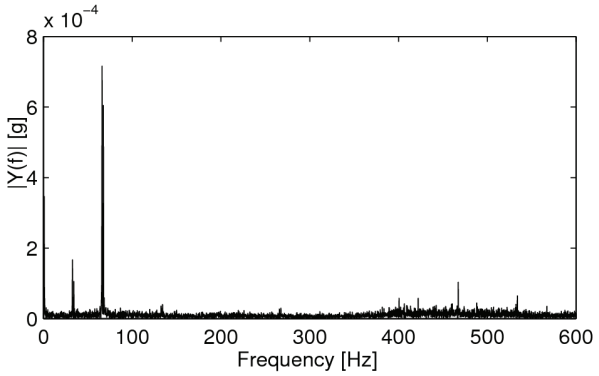

Fig.12. Amplitude spectrum of the measured acceleration in the radial direction at the frame at the end A

The frequency responses of the stator using AMB currents for radial directions are presented in Fig. 15. The symbols over the figures indicate the corresponding response function, for example, $\mathbf{G}_{AB}$ is the response from the B end to the A end. The accelerometers are located in the vicinity of the actuation planes of the radial AMBs. The stator responses contain more resonances than the rotor ones. The rotor responses to the control currents are presented for the reference in Fig. 16. The frequency responses in Figs. 15 and 16 were calculated using joint-input-output estimator [11].

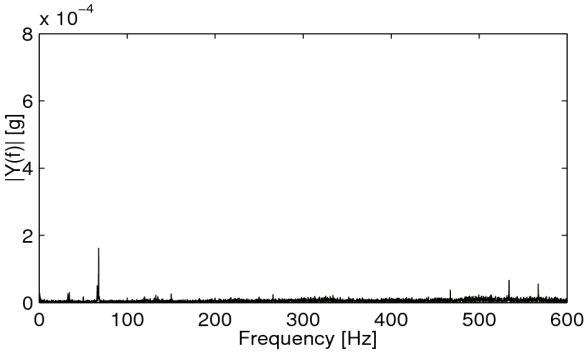

Fig.13. Amplitude spectrum of the measured acceleration in the radial direction at the frame at the end B

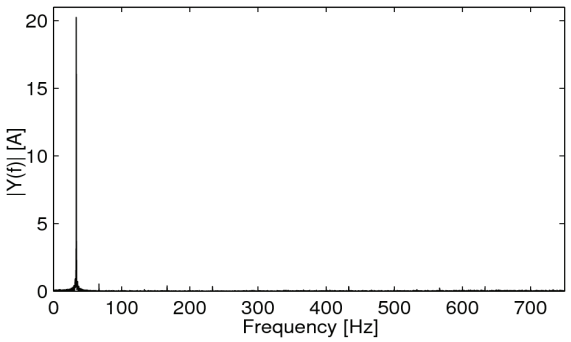

Fig.14. Amplitude spectrum of the measured real component of the stator current

Figure 17 shows the rotor responses to the drive currents. First, the maximum signal amplitude is about 28 times smaller than the maximum amplitude in Fig. 11. Second, the highest amplitude peeks are visible at frequencies around 50 Hz. Additionally the 300 Hz and 150 Hz vibrations are visible. In fact, in Fig. 17 can be seen also a rotor response to the white noise excitation and the characteristic pattern of rotor resonances and antiresonances as presented in Fig. 16. Finally, the vibrations of the same frequency as the frequency of the drive currents are shown.

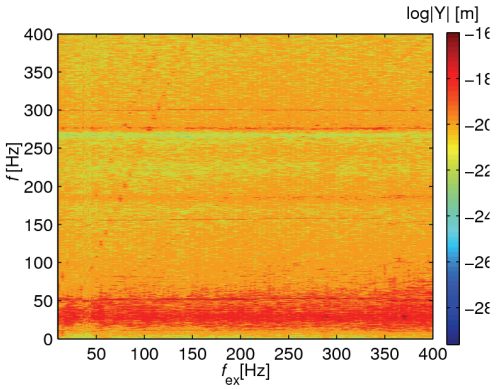

Fig.17. Rotor response to the drive currents (excitation frequency f_{ex} with 5 Hz resolution) at the end A in *x* direction

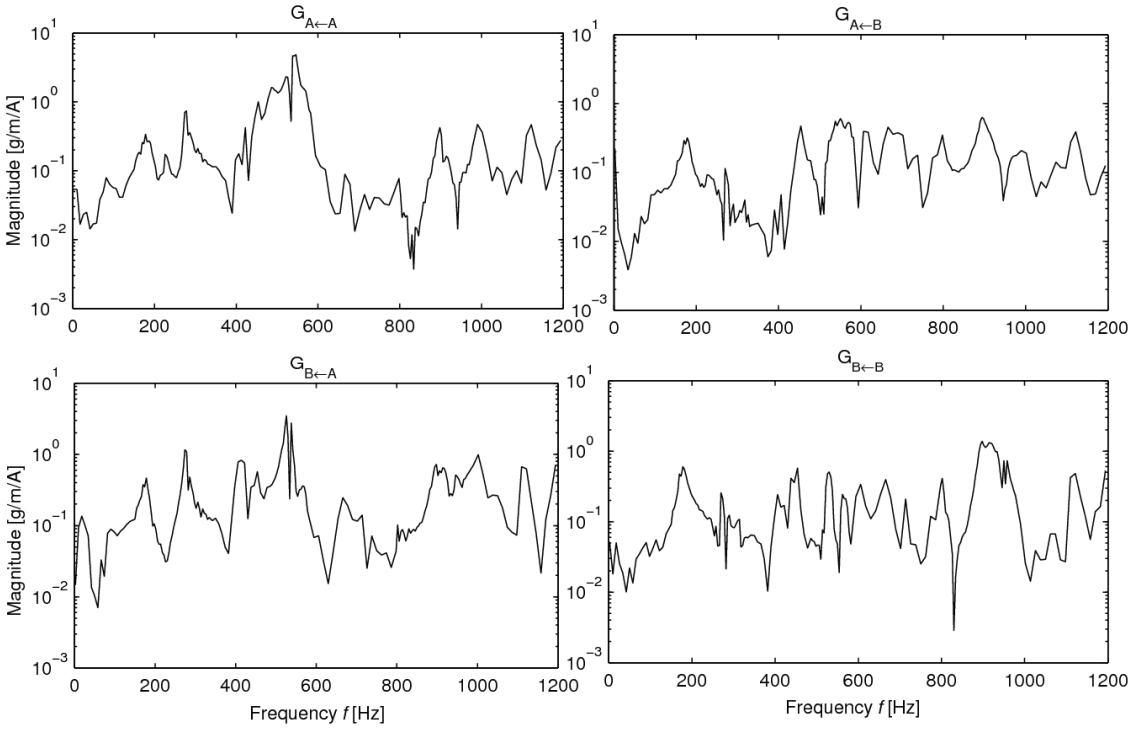

Fig.15. Stator frame response to the control currents

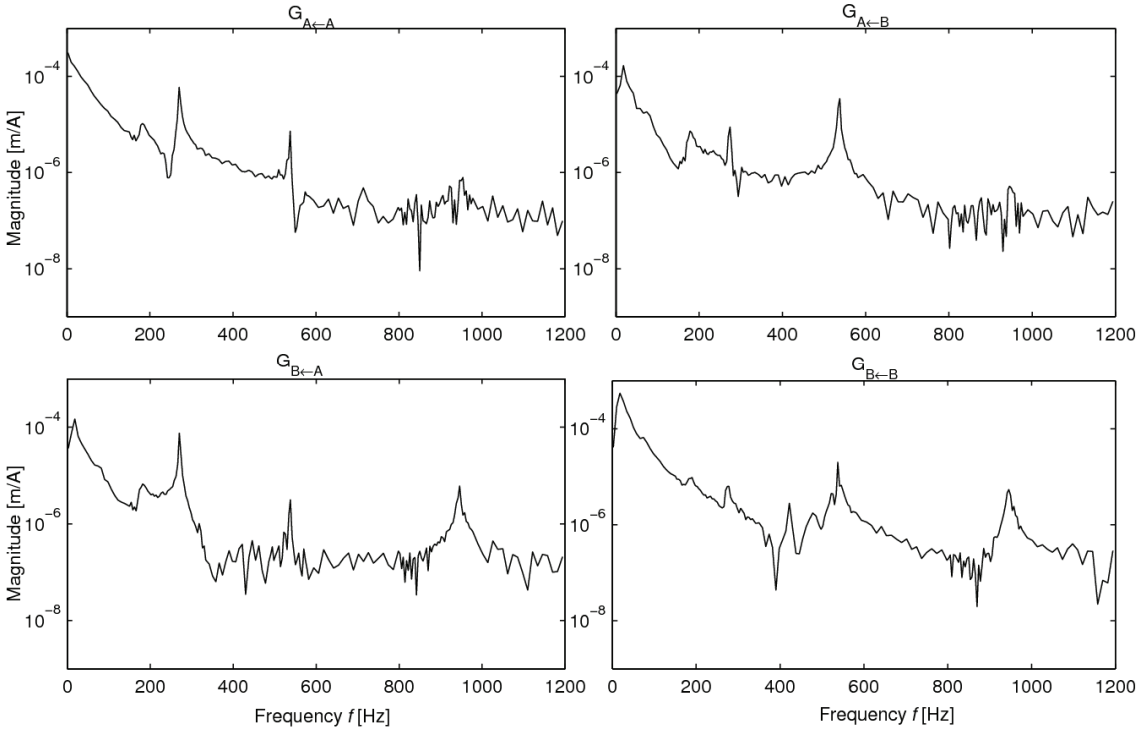

Fig.16. Rotor response to the control currents

Conclusions

The AMB dc link voltage ripple modulates the sinusoidal control currents applied by the controller and might deteriorate the system stability by exciting the mechanical resonances at low frequencies. The amplitudes of the resulting low frequency vibrations are significant. The voltage ripple can be reduced by increasing the dc link capacitance, filtering or including the voltage measurement in the AMB control.

The level of the white noise is increased in the presence of the drive currents. The influence on the axial suspension is weaker than on the radial one because the measurements of the axial suspension are located further from the terminal of the phase currents and source of disturbances.

Additionally, based on the measured responses it is possible to construct the frequency models of the

disturbances entering to the plant and apply them to the *H*-infinity control design.

The obtained results help in better understanding of the limitations in the AMB rotor system. The results will provide guidance for the system, hardware and control designers. The construction of better system models and design of more robust controllers with respect to the known disturbances will be possible. After studding the effect of the drive, the continuation of the work will focus on the influence of disturbances generated by the motor on the AMB control system. The machines with the induction motor and with the permanent magnet motor will be investigated. The voltage measurement will be included in the AMB control to minimize the effect of the AMB dc link voltage variations.

REFERENCES

[1] Schweitzer G., Maslen E.H., Editors (2009), Magnetic Bearings: Theory, Design, and Application to Rotating Machinery, Springer, New York.

[2] Schweitzer G., Active magnetic bearings – chances and limitations, in: Proc. of IFToMM, 2002.

[3] Xu, L., Zhang, J., A study on high temperature displacement sensor. IEEE Trans. on Instrumentation and Measurement (2000).

[4] Burdet L. (2006), Active magnetic bearing design and characterization for high temperature applications. PhD thesis, EPF Lausanne.

[5] Jiang K., Zhu, C. Multi-frequency periodic vibration suppressing in active magnetic bearing-rotor systems via response matching in frequency domain, *Mechanical Systems and Signal Processing* 25 (2011) 1417–1429.

[6] ISO Standard 14839-4. Mechanical vibration - Vibrations of rotating machinery equipped with active magnetic bearings - Part 4: Technical guidelines, system design (Draft), 09 2006.

[7] Jastrzebski R.P. (2007), Design and Implementation of FPGA-based LQ Control of Active Magnetic Bearings, Dissertation, LUT, Finland.

[8] Jastrzebski R.P., Hynynen K., Smirnov A., H-infinity control of active magnetic suspension, *Mechanical Systems and Signal Processing* 24 (2010) No. 4, 995–1006.

[9] Pejovic P. (2007), Three-Phase Diode Bridge Rectifier with Low Harmonics Current Injection Methods, Springer, Ch. 2.

[10] Luukko J., Niemelä M., and Pyrhönen J., Estimation of the flux linkage in a direct-torque-controlled drive, *IEEE Trans. Ind. Electron.* 50, (2003) 283–287.

[11] Ljung L. (1999), System identification: theory of the user, Englewood Cliffs, NJ: Prentice-Hall, 2nd edn.

***Authors**: Dr Rafał P. Jastrzębski, MSc Katja Hynynen, MSc Alexander Smirnov, Prof. Olli Pyrhönen, Dept. of Electrical Engineering, LUT Energy, Lappeenranta University of Technology, PO 20, 53851 Lappeenranta, Finland, e-mails: rafal.jastrzebski@lut.fi, katja.hynynen@lut.fi, alexander.smirnov@lut.fi, olli.pyrhonen@lut.fi*